Engineering Structures 81 (2014) 432–443

Contents lists available at ScienceDirect

Engineering Structures

journal homepage: www.elsevier.com/locate/engstruct

Identification of dynamic displacements and modal frequencies of a medium-span suspension bridge using multimode GNSS processing

Jiayong Yu [a,b], Xiaolin Meng [b,*], Xudong Shao [a], Banfu Yan [a], Lei Yang [b]

[a] College of Civil Engineering, Hunan University, Changsha 410082, Hunan, China
[b] Nottingham Geospatial Institute, the University of Nottingham, Nottingham NG7 2TU, UK

ARTICLE INFO

Article history:
Received 31 December 2013
Revised 24 July 2014
Accepted 6 October 2014
Available online 28 October 2014

Keywords:
Medium-span bridge
Global Navigation Satellite System
Dynamic displacements
Vibration frequencies
Multimode adaptive filter
Accelerometer

ABSTRACT

Global Navigation Satellite System (GNSS) positioning technology has been employed in the dynamic monitoring of long-span bridges in the recent years. However, it has difficulties to meet the higher accuracy requirements of the dynamic monitoring of small or medium span bridges, due to the presence of measurement noise from multipath, cycle slips, ionosphere delay, orbital errors, etc. To verify the feasibility of using current GNSS technology to monitor these bridges, a series of monitoring experiments have been carried out on the Wilford suspension bridge in Nottingham (UK) with GNSS and a triaxial accelerometer. Three GNSS data processing modes, i.e. Real-Time Kinematic (RTK), network RTK and Post-Processing Kinematic (PPK), were considered. An innovative multimode adaptive filtering (MAF) that combining adaptive filter with Chebyshev highpass filter was used to identify the dynamic displacements of the bridge from the multimode GNSS data. To validate the GNSS results, the dynamic displacements were also computed from double integration of the accelerometer-measured accelerations. The differences of the displacements between the GNSS and accelerometer results were obtained. The standard deviation and the mean deviation of these differences are less than 1 mm, which is good enough for the monitoring purposes. The modal frequencies of the bridge can be accurately identified from GNSS measurements, and successfully validated by those from the accelerometer data. Using the multimode GNSS data and the proposed the MAF algorithm, with sub-millimeter level accuracy GNSS can be used to monitor the vibration response of small or medium span bridges as well as long-span bridges.

1. Introduction

Global Navigation Satellite System (GNSS) positioning technology, as an innovative monitoring method for the dynamic response of engineering structures, has many attractive advantages over other traditional monitoring methods. These advantages include provision of real-time 3D absolute displacements of engineering structures, continuously autonomous operation under all weather conditions, data acquisition with no need for line-of-sight between different stations [1]. GNSS technology can overcome some shortcomings of the accelerometer method, which has difficulties to continuous monitoring of engineering structures, and to monitor slow structural vibration with a frequency of less than 0.2 Hz [2–4]. Other techniques for structural health monitoring, such as terrestrial positioning systems, laser displacement sensors, and photo/video imaging methods, have received attentions, but still have limitations such as weather dependency and short monitoring distance (in the order of a few hundreds of meters) [5,6].

Currently technology based on GNSS systems, which include GPS, GLONASS, Galileo (under construction) and BeiDou Navigation Satellite System (BDS, under construction) [7], has been successfully applied to the dynamic monitoring of tall buildings and long-span bridges, due to its overall significantly improved performance and high data sampling rate. The pioneer studies on GNSS-based structural health monitoring started in mid 1990s. Lovse et al. [8] reported a specific application of using GNSS receivers to monitor the dynamic displacements of the Calgary Tower in Alberta, Canada, which successful monitor the dynamic displacements of around 16 mm with the fundamental frequency of 0.36 Hz on the tower. Ashkenazi and Roberts et al. [9] illustrated the experiments of using kinematic GNSS technique to monitor the dynamic response of the Humber Bridge in United Kingdom. They demonstrated that the GNSS technology can be used to determine the deformation characteristics of the bridges in real-time. These successes motivated the applications of the GNSS technology in the dynamic monitoring of large engineering structures

* Corresponding author.
E-mail addresses: surveying@hnu.edu.cn (J. Yu), xiaolin.meng@nottingham.ac.uk (X. Meng).

http://dx.doi.org/10.1016/j.engstruct.2014.10.010
0141-0296/

(Breuer et al. [10]; Ge et al. [11]; Xu et al. [12]; Tamura et al. [13]; Kijewski-Correa et al. [14]; Yigit et al. [15]; Watson et al. [16]; Roberts et al. [17]; Meng [18]; Li et al. [19]; Yi et al. [20]; Moschas and Stiros [21]). Meanwhile, experiments had been conducted to assess the performance of the GNSS technology. For instance, Meng et al. [18] had conducted a series of zero baseline and short baseline experiments to evaluate the performance of the GNSS receivers, in which the characteristics of the GNSS measurements noise were analyzed. Nickitopoulou et al. [22] summarized a series of experiments made on a rotating prototype device to define that the GNSS technique can monitor the displacements smaller than 15 mm, at a 1.5% outlier level. For the first time, Yi et al. [23] assessed the performance of high-rate GNSS receivers through the simulated and the full-scale experiments, and illustrated that receivers at a sampling rate of 50 Hz or 100 Hz, could identify the high structural vibration frequencies of up to 10 Hz. Other researches for assessing the performance of the GNSS technology had been performed by Kijewski-Correa et al. [5], Roberts et al. [24], Chan et al. [25], Moschas and Stiros [26,27], etc. In conclusion, the researches demonstrated that the GNSS techniques can trace the dynamic displacements of tall buildings and long-span bridges with satisfactory results (for summary reviews see [6,28,29]).

GNSS monitoring has inherent erroneous sources. Some errors (ionospheric and tropospheric delays, and orbital errors) can be mitigated greatly with double-differencing over short baselines (e.g., shorter than 10 km). Some other errors, such as multipath error and random noise, cannot be removed in the differencing method [30]. Several data processing techniques could be performed to mitigate these residual errors, such as an adaptive filtering (AF) technique [31–33], a technique combining Empirical Mode Decomposition (EMD) and AF [34], an improved particle-filtering algorithm [35], a supervised learning technique [36], and a wavelet based multi-step filtering method [37]. In summary, most of the current filtering techniques can identify centimeter level displacements with a millimeter level accuracy. However, GNSS positioning technology has difficulties in monitoring the dynamic displacements of small or medium span bridges with high accuracy, although there are some cases of monitoring these types of bridges [2,4,21]. The main reason is that for the small or medium span bridges the vibration displacements is in the millimeter level, which is buried in the GNSS measurement errors, such as multipath effect, cycle slips, ionosphere delay, etc [38].

To address the problems encountered when applying GNSS technology to monitoring the dynamic response of small or medium span bridges, this study proposed a multimode data acquisition approach and a multimode adaptive filtering (MAF) algorithm to identify the dynamic displacements of these bridge with GNSS sensors with sub-millimeter level accuracy. GNSS data with three processing modes, i.e. conventional Real-Time Kinematic (RTK), network RTK, and Post-Processing Kinematic (PPK) were obtained in the experiments conducted on the Wilford suspension bridge in Nottingham, United Kingdom. A Precise Time Data Logger (PTDL) and a special cage were manufactured to solve two key implementation problems, which are the time synchronization and the axis alignment between two types of sensors, respectively. The MAF algorithm, which combines the Chebyshev highpass filter with adaptive filter, was used to mitigate the GNSS measurement errors. The dynamic displacements of the bridges were identified from the multimode GNSS data using the proposed MAF algorithm. The accelerometer data was acquired with the PTDL data logger to assess the accuracy of GNSS results. The identified displacements and frequencies from GNSS technique were compared with those from the accelerometer technique, which is used as a reference solution.

This study demonstrates that the dynamic displacements of this medium-span bridge, which are in the level of a few millimeters, could be identified accurately *at sub-millimeter level accuracy* from the multimode GNSS data by the proposed MAF algorithm. The fundamental frequency of the bridge also can be extracted from the multimode GNSS data with the Fast Fourier Transform (FFT). Although this study is only focused on the vertical displacement, it also can also be used to analyze the horizontal deformation, since the GNSS measurements are more accurate in the horizontal directions [1].

2. The Wilford suspension bridge in Nottingham

The Wilford suspension bridge is an earth-anchored suspension footbridge that is supported by two main cables over the River Trent in Nottingham, United Kingdom (Fig. 1). It was constructed in 1904 with a single span of 69 m long and 3.7 m wide. However, this Grade Two listed bridge had to be closed to ensure the safety of the general public because of debris falling down from the bridge in 2008. It was reopened in 2010 after its owner, Severn Trent Water, reinforced the main beams and replaced the defective steel components and fixings.

The researchers of the University of Nottingham utilized the bridge as a testbed for two monitoring projects supported by the UK's Engineering and Physical Sciences Research Council (EPSRC), and the European Space Agency (ESA), respectively. They had conducted numerous in-situ monitoring experiments on this bridge in the last ten years using different sensors and approaches. For instance, a GNSS augmented with pseudolites system was employed in the dynamic monitoring of this bridge, with an improved accuracy of several millimeters [1]. A frequency peak-picking approach was developed to successfully detect the vibration frequencies of this bridge from the GNSS data [2]. A high-rate JNS100 GNSS receiver was used to monitor deflections of this bridge, but most movement on the bridge was masked by the GNSS noise [24]. A monitoring trial was conducted on this bridge using a Leica TCA2003 robotic total station, and the results indicated that the total station had many difficulties measuring structural dynamic displacements [39]. In addition, structural analysis has been performed according to the field measurements on the bridge structure, member size, as well as the material characteristics, and the fundamental frequency 1.74 Hz of the bridge is obtained by the numerical analysis [40].

Nevertheless, due to the restoration, the dynamic parameters of the bridge structure are different from those in the past, and cannot be computed accurately using numerical analysis. Therefore, it is necessary to re-measure/identify the dynamic parameters of the bridge for the purpose of assessing the bridge performance. We conducted a series of experiments once again to measure the dynamic displacements and modal frequencies of this bridge. These latest experiments are different from the past ones conducted on the same bridge, because we synchronously considered three GNSS data acquisition modes, and employed the latest generation of GNSS receivers. All the data sets were processed with a newly developed algorithm – MAF, which will be explained in details in the following section.

3. Field experiments

The field experiments were conducted on the Wilford suspension bridge in Nottingham, United Kingdom in June and August 2012, throughout which the weather was fine. The aim of the experimental study was (1) to identify the dynamic displacements and modal frequencies of the bridge with GNSS sensors, in which three different GNSS data modes, i.e. conventional RTK, network RTK and PPK were considered, and (2) to verify the accuracy and

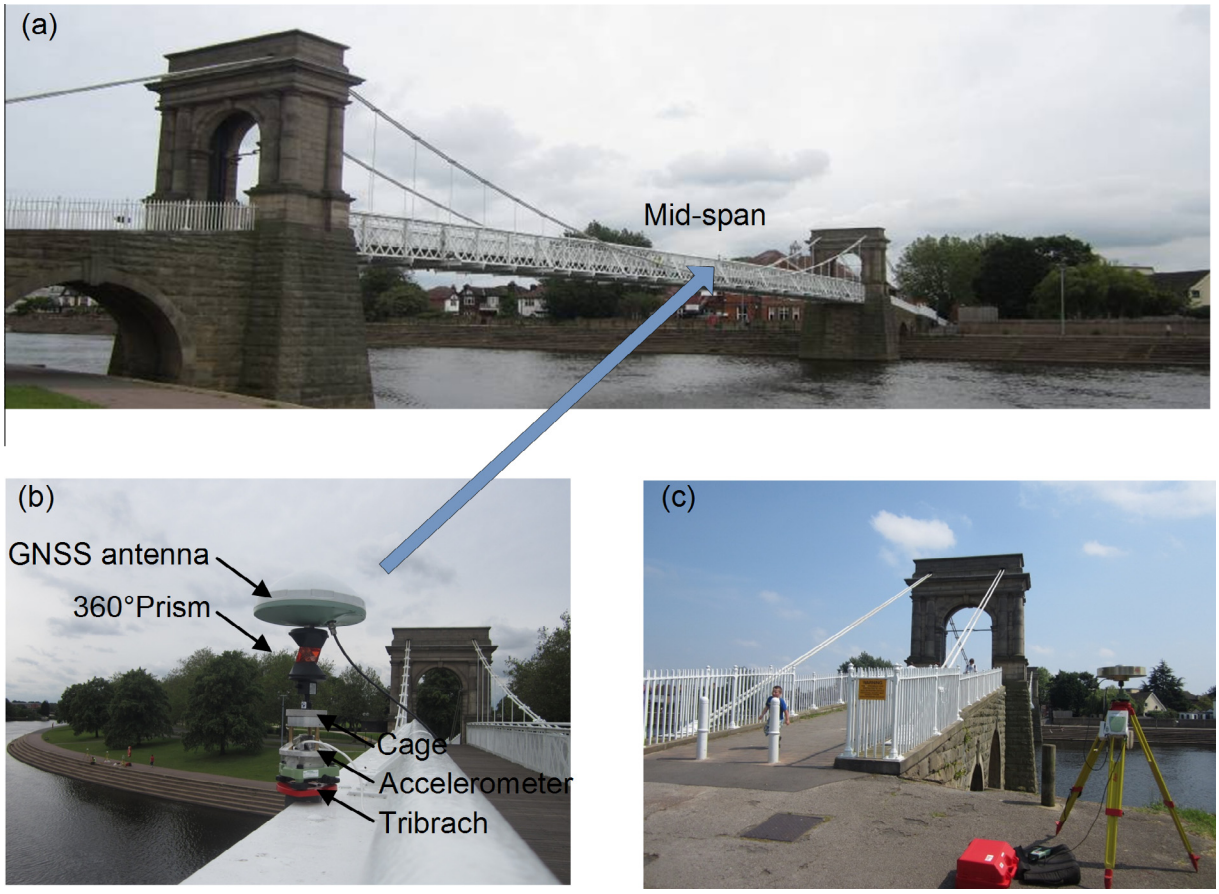

Fig. 1. View of the medium-span Wilford suspension bridge in Nottingham and instrumentation. The monitoring devices were fixed on the handrail (b), located in the mid-span of the bridge (a). The GNSS receiver of the local reference station was set near the bridge (c).

effectiveness of the innovative MAF algorithm by analyzing experimental results of the GNSS and accelerometer sensors.

3.1. Instrumentation

The main instrumentation employed in the experiments includes three sets of GNSS sensors, a tri-axial accelerometer, a PTDL data logger, and a special cage. Although a Leica TS30 robotic total station is also used to monitor dynamic responses of the bridge, this content is beyond the scope of the paper.

3.1.1. GNSS receivers

We used three sets of GNSS sensors consisting of three dual frequency Leica GS10 receivers with the sampling rate of up to 20 Hz, a Leica AR10 antenna and a LEICAT504 choke-ring antenna. An accuracy of a few millimeters for short baseline can be obtained with these GNSS sensors, which have been successfully assessed and verified in the past experiments [5,18,25]. The choke-ring antennas were employed to reduce the multipath error, which is one of the main error sources for the GNSS stations (close to water, metal or other reflecting surfaces such as piers, cable and the deck of the suspension bridge) [22]. The LEICAT504 choke-ring antenna was used on the reference station, and the AR10 antenna was used on the mobile rover station (monitoring site) that offers near choking-ring level performance but with much reduced weight and size.

3.1.2. Triaxial accelerometer

We used a Kistler K-BEAM 8392A2 triaxial accelerometer with a sampling rate of up to 150 Hz and an acceleration range of ±2 g. The accelerometer is ideal for the modal test of large structures because it can measure acceleration in three mutually perpendicular axes (x, y, z) with low noise and high sensitivity [2,38].

3.1.3. PTDL data logger

When the integrated GNSS and accelerometer system was used for structural dynamic monitoring to improve measurement accuracy and measureable frequency range [3,34,38,41], it has a key difficulty of time synchronization. To solve this problem, a Precise Time Data Logger PTDL (see upper-right of Fig. 2), which is recently developed by the researchers of the University of Nottingham, was used to record the accelerometer data in true GNSS time. It is composed of core logger chip, an external power supply, and a low-cost GNSS antenna. The core logger chip contains a storage memory and a built-in low-cost GNSS chip, which tags GNSS time onto the external data from the accelerometer. Meanwhile, the data themselves from the GNSS receivers contain precise GNSS time. therefore, the data from both sensors can be used for further study such as data comparison and data fusion based on the same GNSS time frame.

3.1.4. Special cage

To solve another key difficulty of axis alignment, the experiments used a special cage at the monitoring site to ensure a rigid vertical axis alignment between the GNSS receiver and the accelerometer. Fig. 1b shows that the GNSS antenna, 360° prism, a special cage and tribrach were consecutively connected, and the accelerometer was installed inside the cage. The cage had two rotatable plates on both ends, connected by three bolts. The North mark of the GNSS receiver was orientated to the north by rotating the

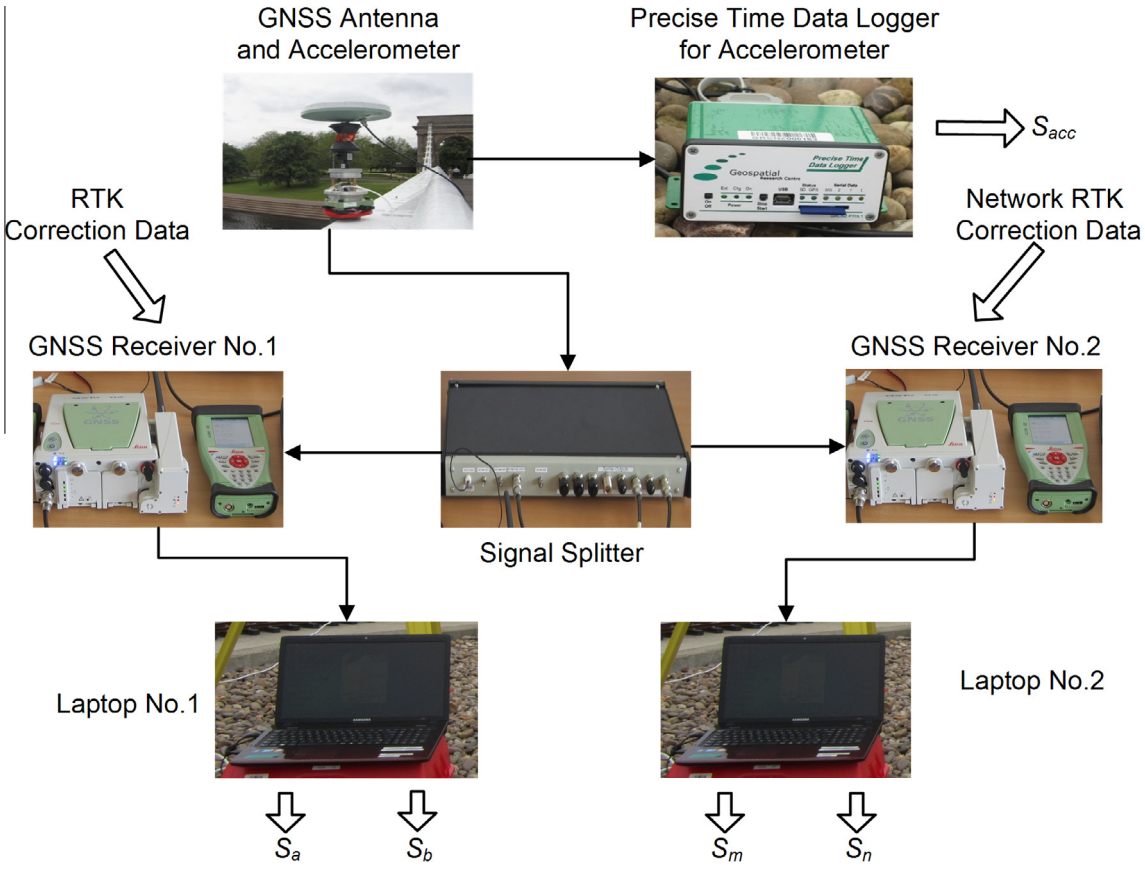

Fig. 2. Synchronously acquiring data from the GNSS and accelerometer sensors at the monitoring site. The GNSS data of conventional RTK (S_a), network RTK (S_m) and PPK (S_b, S_n) were synchronously acquired via a signal splitter, and accelerometer data (S_{acc}) was acquired via a Precise Time Data Logger.

upper plate. Meanwhile, one axis of the accelerometer was aligned with the longitudinal axis of the bridge by rotating the lower plate. When the tribrach is leveled, the GNSS antennas, the prism, the accelerometer, and the tribrach are in the same vertical axis.

3.2. Multimode data acquisition

In past ten years, the application of GNSS positioning technology in monitoring the dynamic responses of bridges mainly focus on using the conventional RTK and PPK methods [4,17,22,23]. The network RTK method was firstly proposed to enhance the RTK performance for structural health monitoring in 2006 [3]. It was initially employed in monitoring dynamic response of a bridge by authors in 2011 [42]. As a further study, we designed a data acquisition approach to obtain multimode GNSS data in three modes, i.e. RTK, network RTK and PPK. As shown in Fig. 2, in order to obtain GNSS data to implement multimode processing, two GNSS rover receivers (No. 1 and No. 2) were connected to the same antenna via a signal splitter. While the No. 1 receiver acquired data (S_a) using conventional RTK mode, the No. 2 GNSS receiver acquired synchronous data (S_m) using network RTK mode. These two rover receivers also recorded the GNSS raw observations into the embedded memory cards, which were post-processed in kinematic mode (so-called PPK) with the professional software – Leica Geo-Office (LGO) to resolve the displacement data (S_b, S_n).

3.3. Experimental procedure

The GNSS positioning technology with three data processing modes (RTK, network RTK and PPK) was apply to monitoring dynamic displacements and modal frequencies of the Wilford bridge in 2012. The GNSS receivers with network RTK mode receives correction differences from the continuously operating reference stations (CORS) whilst a conventional RTK uses correction data from a local reference station. The CORS services have been provided in United Kingdom since 2006, whilst many countries have provided similar services [43]. The No. 11 station of the UK's CORS, which locates in Keyworth, Nottinghamshire, is the closest reference station to the monitoring site about 7.4 km away. Hence, it is utilized as the master reference station, and the others nearby as auxiliary reference stations for producing network RTK solutions. The CORS network transmitted the real-time corrections with an interval of 1 s for the network RTK solution.

The local reference station was also set up on a stable location close to the bridge, where No. 3 GNSS receiver and the LEICAT504 antenna were installed (Fig. 1c). This reference receiver transmitted real-time corrections with an interval of 1 s for the conventional RTK solution, and recorded the raw observations with a sampling rate of 20 Hz. The monitoring site was set at the downstream (south) side of the mid-span of the bridge, where an AR10 GNSS antenna and an accelerometer were fixed on the bridge handrail (Fig. 1b). Two GS10 GNSS rover receivers (No. 1 and No. 2) were connected to the same antenna via a signal splitter. Four sets of GNSS data were obtained from the GNSS measurements, i.e. RTK data (S_a), network RTK data (S_m) and PPK data (S_b, S_n) as shown in Fig. 3. The PPK data of S_b and S_n are not the same because the random noise (instrument self-noise) between them are different. A pair data selected from these multimode data (S_a, S_b, S_m, S_n), as shown in Table 1, will be used as the input data and the desired data, respectively, to implement multimode adaptive filtering.

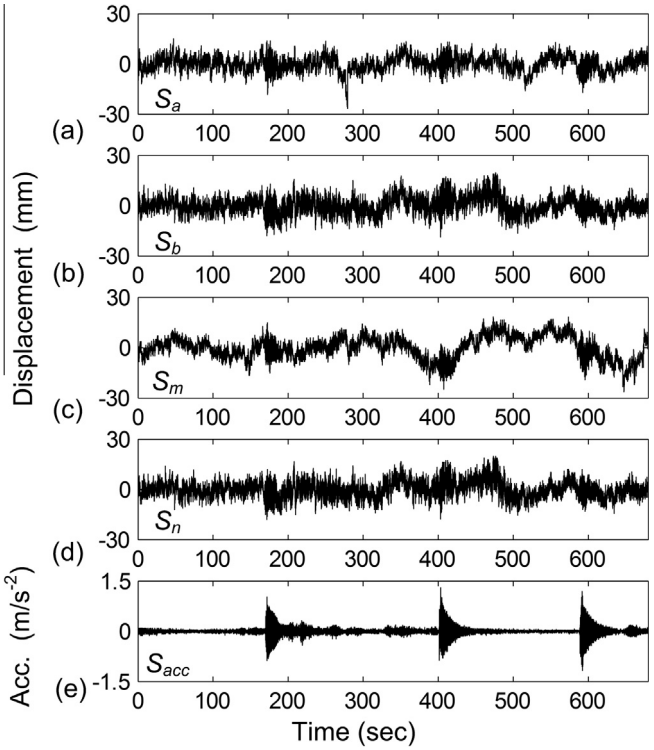

Fig. 3. Time series of dynamic response of the bridge derived from GNSS and accelerometer records. The displacements with RTK (a) and PPK mode (b) were derived from the No. 1 GNSS receiver records, and those with network RTK (c) and PPK mode (d) were derived from the No. 2 GNSS receiver records. The time series of acceleration (e) was acquired from the accelerometer.

It is noted that the corrections are transmitted from the local reference station or the CORS network only at the updating rate 1 Hz. The reason is that the GNSS hardware can not transmit the corrections at a very high frequency. Fortunately, the updating rate 1 Hz is enough for the RTK solution at the sampling rate 20 Hz because the change of corrections is relatively slow. All GNSS sensors received GPS and GLONASS satellite signals in 4th case, whereas they received only GPS satellite signals in other cases (Table 2), with an elevation cut-off angle 15°. The professional software – Leica Geo-Office (LGO) for window version 7.0 was employed in resolving the baseline in kinematic mode (So-called PPK). The limitation of Geometric Dilution of Precision (GDOP) was set as 15. The Hopfield tropospheric model, the Computed ionospheric model and the precise ephemeris data were used for the PPK solution. The precise ephemeris data were freely downloaded from the website (http://garner.ucsd.edu/pub/products/1780/).

Besides, the tri-axial accelerometer was installed on a special cage (Fig. 1b), whose *z*-axis was aligned with the vertical axis of the GNSS antenna, and *x*-axis was parallel to the bridge longitude axis. Accelerations (S_{acc}) were recorded and synchronized with GNSS measurements using the PTDL (Fig. 3e). With this above configuration four sets of vibration data with the sampling-rate of 20 Hz were synchronously produced by the GNSS receivers and the fifth data with 100 Hz by accelerometer. The configuration used for this data acquisition procedure is summarized in Table 1.

Table 1
Synchronous acquired GNSS and accelerometer data.

Data	Instrument	Mode	Type	Sample-rate
S_a	GNSS No. 1	RTK	Displacement	20 Hz
S_b	GNSS No. 1	PPK	Displacement	20 Hz
S_m	GNSS No. 2	Network RTK	Displacement	20 Hz
S_n	GNSS No. 2	PPK	Displacement	20 Hz
S_{acc}	Accelerometer	\	Acceleration	100 Hz

Five case studies with different force conditions were conducted in the field experiments (Table 2). The forced vibrations of the bridge were excited by a group of three people with a total weight 180 kg at its mid-span. These people synchronously or asynchronously jumped around 10 s each time with an interval of 3 min. Ambient random vibrations of the bridge were measured, which may be caused by the wind and occasional pedestrian loads. During field experiments, pedestrians and bicyclists traveled across the footbridge occasionally, and the environmental temperature changed in the range of 20.4°–21.0° with gentle southwest wind. We selected and analyzed the GNSS and accelerometers data covering approximately 70 min in case 1, in which three people synchronously jumped on the bridge. However, in order to focus on the details, we only presented 680 s data in the following section, which were synchronously acquired from 10:15:40 am to 10:27:00 am on 3rd August 2012.

4. Multimode adaptive filter – MAF

Most of the current filtering techniques can identify centimeter level displacement with a millimeter level accuracy. However, it is difficult to detect the dynamic displacements in millimeter level from the background noise in the GNSS measurements. For the purpose of identifying millimeter level amplitude vibration of the small or medium span bridges, we developed an innovative MAF algorithm to distinguish the actual vibration information ($V(n)$) from the background noise (Fig. 4). This GNSS measurement noise consists of the multipath error ($M(n)$) which is mainly distributed in a relatively low frequency range of less than 0.2 Hz [20], and the random noise ($N(n)$) which is distributed in a broad frequency range with the characteristics of both the white and colored noise. These characteristics of the background noise in GNSS measurements had been illustrated by many researchers [5,23,44].

The MAF algorithm combined a Chebyshev highpass filter with an adaptive filter to mitigate the main GNSS measurement errors, and to identify the dynamic displacements from a pair of GNSS data. The principle of the adaptive filter have been illustrated in detail by Ge et al. [45] and Haykin [46]. A pair of GNSS data (S_a, S_b) as shown in Fig. 5a and b, which contained the information of the dynamic response of the experimental bridge at the same site under the same time, was selected from the aforementioned multimode data (S_a, S_b, S_m, S_n) to demonstrate the filtering procedure. Ignoring the secondary noise in GNSS measurements, such as the residual of orbital errors that was mitigated greatly with double-differencing over short baselines [30], the pair of data can be expressed as

$$S_a = M_a(n) + V_a(n) + N_a(n) \quad (1)$$

$$S_b = M_b(n) + V_b(n) + N_b(n) \quad (2)$$

where n is the length of the time series of the vibration data; $M_a(n)$ and $M_b(n)$, corresponding to the GNSS data of S_a and S_b, respectively, are relatively low frequency component, which is mainly consist of the multipath error; $V_a(n)$ and $V_b(n)$ are the actual dynamic displacements of the bridge; $N_a(n)$ and $N_b(n)$ are random noise (white and colored noise [44]). The filtering procedure includes two steps (Fig. 4). At the first step the relatively low frequency components of $M_a(n)$ and $M_b(n)$, mainly caused by the multipath effect, were eliminated by the designed Chebyshev highpass filter. At the second step, taking advantage the strong correlation of the pair of GNSS data, the random noise $N_a(n)$ was greatly mitigated and the actual vibration information $V_a(n)$ could be extracted by the adaptive filter.

Table 2
Description of five experimental cases.

Case	Description
1	Three people (180 kg in total) jumped synchronously. GNSS receivers acquired GPS signal
2	Three people jumped asynchronously. GNSS receivers acquired GPS signal
3	No jumping, wind and Occasional pedestrians. GNSS receivers acquired GPS signal
4	Three people synchronously jumped. GNSS receivers acquired GPS and GLONASS signal
5	No jumping, wind and Occasional pedestrians. GNSS receivers acquired GPS signal

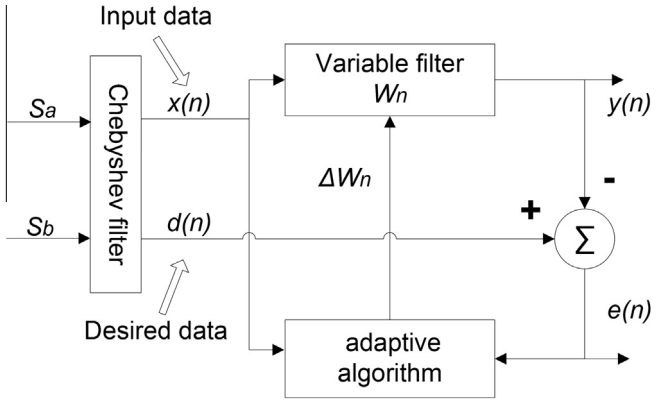

Fig. 4. Filtering procedure of multimode adaptive filter MAF.

First, to eliminate the low frequency components ($M_a(n)$, $M_b(n)$), we applied a Chebyshev highpass filter to eliminate the low frequency components ($M_a(n)$, $M_b(n)$) with a frequency range of less than 0.2 Hz [20], which is similar to the previous Chebyshev filter discussed in Ref. [2], whose passband cut-off frequency is chosen on the basis of the structural analysis. Here, we chose an 8-ordered Chebyshev highpass filter with passband frequency of 1.0 Hz, because the fundamental frequency of the Wilford bridge is around 1.74 Hz from the previous structural analysis [40]. The Chebyshev filtered results ($x(n)$, $d(n)$), as shown in Fig. 5c and d, mainly consist of actual dynamic displacements ($V_a(n)$, $V_b(n)$) and random noise ($N_a(n)$, $N_b(n)$) after the elimination of the low frequency components ($M_a(n)$, $M_b(n)$), which can be expressed as

$$x(n) = V_a(n) + N_a(n) \tag{3}$$

$$d(n) = V_b(n) + N_b(n) \tag{4}$$

following the above procedures, we applied the Least Mean Square (LMS) adaptive filter to greatly mitigate random noise $N_a(n)$ and identify the actual vibration of the bridge $V_a(n)$. Two time series, i.e. desired data $d(n)$ and input data $x(n)$, are needed to implement adaptive filtering, which are sometimes called the primary input and reference input, respectively. The primary input includes the desired signal plus undesired interference (random noise), whereas the reference input includes the signals that are correlated to some of the desired signal. The input data $x(n)$ and the desired data $d(n)$ contain the actual structural vibration components ($V_a(n)$, $V_b(n)$) as shown in Eqs. (3) and (4), respectively. These actual vibration components ($V_a(n)$, $V_b(n)$), corresponding the multimode data (S_a, S_b) as shown in Eqs. (1) and (2), are identical because they are obtained from the structural vibration occurred at the same site under same instant. The random noise of $M_a(n)$ and $M_b(n)$ do not correlate. Then, we utilized the cross-correlation between the input data $x(n)$ and the desired data $d(n)$, which were the above

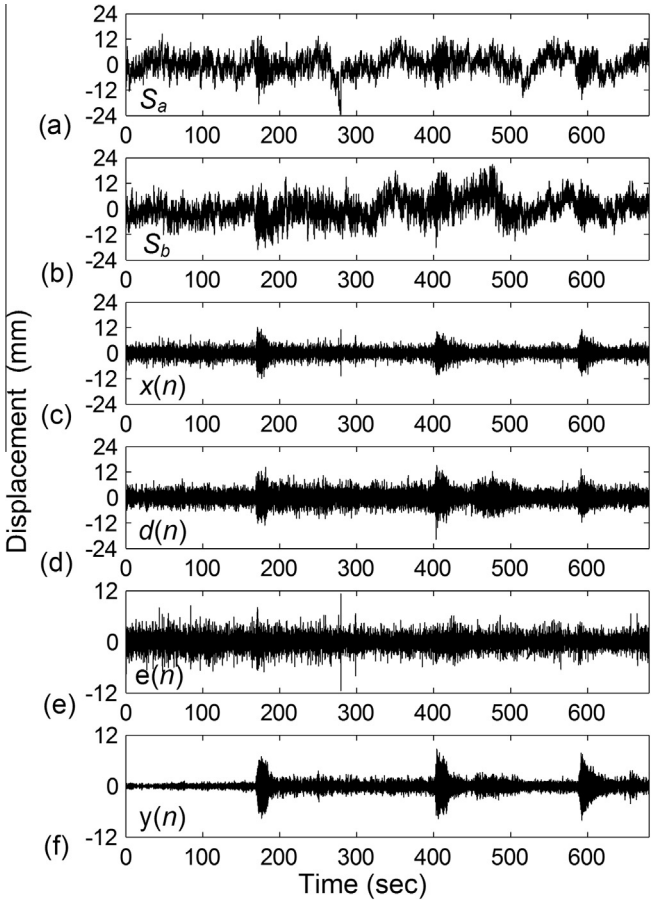

Fig. 5. Filtering results using the multimode adaptive filter MAF. The first step filtering results (c, d) were obtained from the multimode original GNSS data (a and b). The estimation errors (e) and the actual dynamic displacements of the bridge (f) were obtained after the second step filtering.

Chebyshev filtered results, to distinguish the actual vibration information $V_a(n)$ from the random noise $N_a(n)$. The relationship between $V_a(n)$ and $V_b(n)$ can be expressed as

$$V_a(n) = V_b(n) \tag{5}$$

The output data $y(n)$ of the adaptive filtering, as shown in Fig. 5f, is the identified actual dynamic displacements $V_a(n)$. It can be obtained from the equation as [45].

$$y(n) = \sum_{i=0}^{M-1} \widehat{w}_i(n) x(n-i) \tag{6}$$

where M is the length of the LMS adaptive filter and $\widehat{w}_i(n)$ denotes the variable parameters, which are the weighting factors in the LMS adaptive algorithm. The input data $x(n)$ consists of periodical structural vibration component $V_a(n)$, and the random noise $N_a(n)$. Thus, the summation of all $M-1$ segments results the actual structural vibration component $V_a(n)$, due to random noise towards to zero, then

$$V_a(n) = y(n) \tag{7}$$

The estimation error $e(n)$ can be obtained from the equation as

$$e(n) = d(n) - y(n) \tag{8}$$

From Eqs. (4), (5) and (8), random noise $N_b(n)$, as shown in Fig. 5e, can be expressed as

$$N_b(n) = e(n) \tag{9}$$

Using the proposed MAF algorithm, the actual dynamic displacements of the bridge can be accurately identified from the two synchronously acquired multimode GNSS data, both of which are contaminated by the GNSS measurement noise.

5. Data processing and results

5.1. Overall procedure

The flowchart in Fig. 6 summarizes the overall procedure to identify dynamic displacements and modal frequencies of the bridge using the multimode GNSS data and the MAF algorithm. *First*, we preliminarily processed the GNSS and accelerometer data (Table 1), such as coordinate system transformation, outlier clearance, and missing data recovering.

Second, under considering three filtering schemes (A, B and C) with different input data, three sets of dynamic displacements (A_1, B_1, C_1) were identified from the combinations of multimode GNSS data by the innovative MAF algorithm. The dynamic displacements were obtained from the double integration of the accelerations to validate the GNSS results. These three filtering schemes (A, B and C) chose three pairs of GNSS data (S_a and S_b, S_a and S_n, S_m and S_a), respectively. The two time series in each pair are regarded as input and desired data (Table 3). Three set of dynamic displacements (A_1, B_1, C_1) were identified from these three pairs of data by the MAF algorithm, respectively (Fig. 7).

Third, three structural vibration frequencies (A_2, B_2, C_2), corresponding to the results of three filtering schemes, were extracted from the three time series of dynamic displacements (A_1, B_1, C_1) by the FFT, respectively (Fig. 7). These extracted vibration frequencies were validated by the vibration frequencies that extracted from the accelerometer data.

Fourth, the time series of accelerations was computed from the time series of GNSS dynamic displacements (A_1) by double differentiation, and its modal frequencies were also extracted by the FFT. These two results were validated by the corresponding accelerometer results.

Fifth, the dynamic displacements were obtained from GNSS data by Ensemble Empirical Mode Decomposition (EEMD), and also by the MAF separately. We calculated the residuals of accelerometer-derived displacements minus the EEMD-filtered displacements, and minus the MAF-filtered displacements separately. The standard deviations and the mean deviations of these residuals were calculated to assess the accuracy and effectiveness of the MAF.

5.2. Preliminary processing

Five sets of original data of the dynamic response of the bridge were acquired at the same time, which included original GNSS-derived displacements and accelerometer-derived accelerations (Fig. 3). To begin with, the original GNSS data in the geodetic coordinate system, i.e. ETRS89 (WGS84) in UK were transformed into the OSGB36 National Grid coordinate system using the software Grid InQuest for the window version 6.5 developed by Ordnance Survey Great Britain. The types of the input and output data were set as geodetic coordinate, and UK & Ireland coordinate in OSGB36 zone respectively during coordinate translation. The software

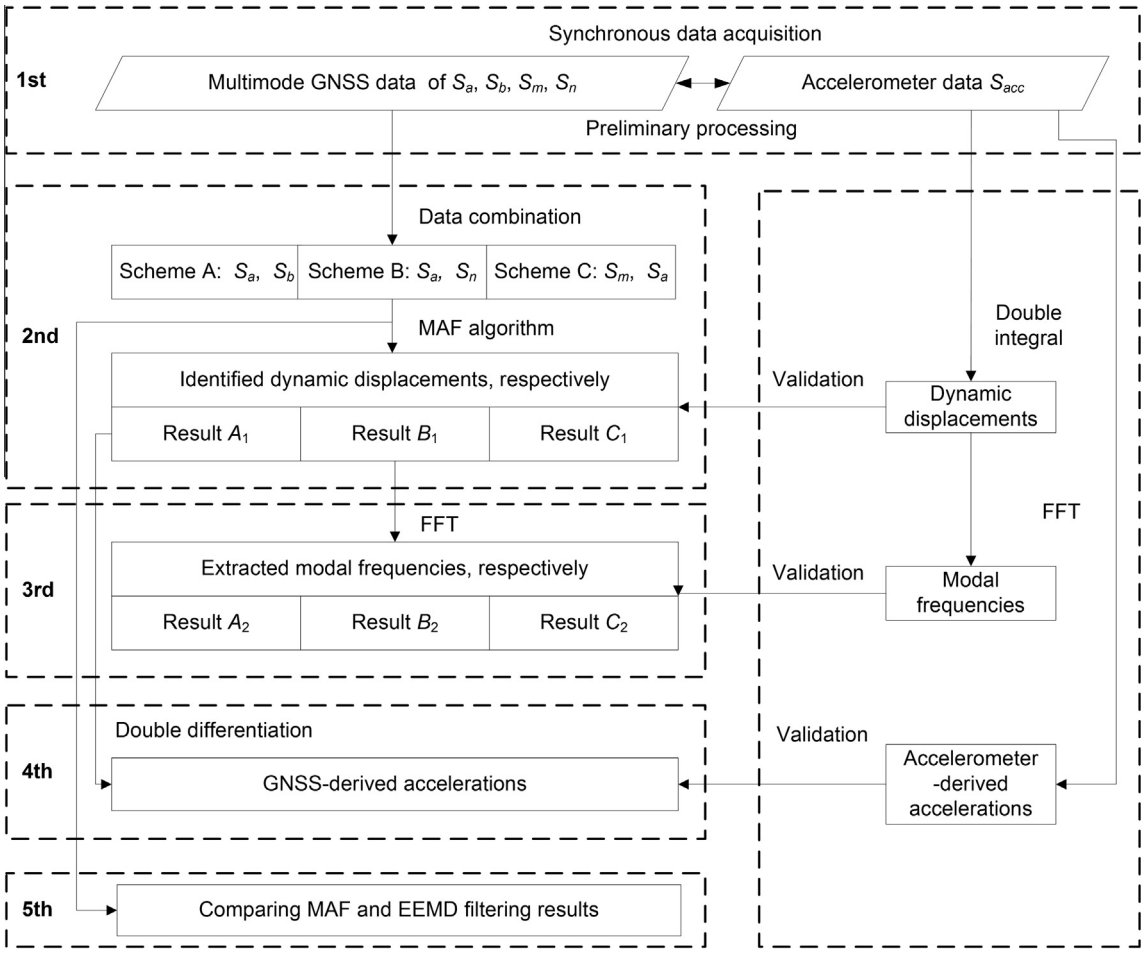

Fig. 6. Flowchart of the procedure to process the GNSS and accelerometer data.

Table 3
Data sources of different schemes.

Scheme		Data	Description
A	$x(n)$	S_a	Conventional RTK data acquired by receiver No. 1
	$d(n)$	S_b	PPK data acquired by receiver No. 1
B	$x(n)$	S_a	Conventional RTK data acquired by receiver No. 1
	$d(n)$	S_n	PPK data acquired by receiver No. 2
C	$x(n)$	S_m	Network RTK data acquired by receiver No. 2
	$d(n)$	S_a	Conventional RTK data acquired by receiver No. 1

Symbol $x(n)$ denotes input data; symbol $d(n)$ denotes desired data.

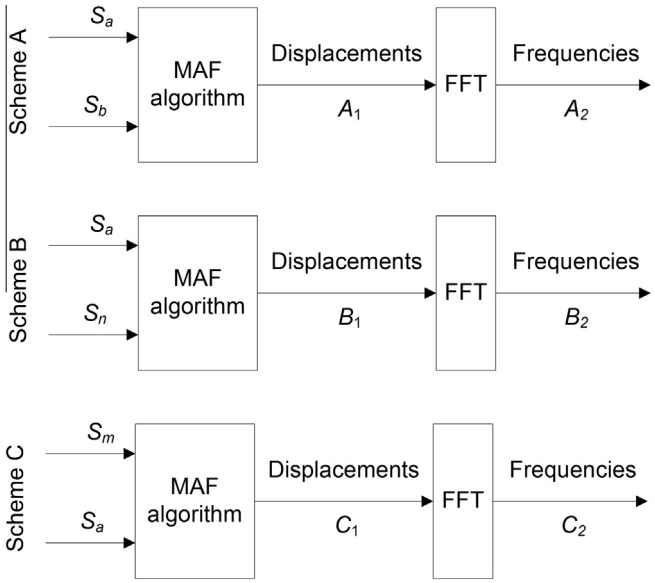

Fig. 7. Processing GNSS data by three filtering schemes.

employed Transverse Mercator (TM) projection to convert ellipsoidal coordinates to plane coordinates. Then, using the rotation matrix (see Ref. [38]), the plane GNSS coordinates were projected onto the bridge coordinate system which has been used in the accelerometer measurements. In the bridge coordinate system, the x-axis and the y-axis were aligned with the longitude and the lateral of the bridge, respectively. Furthermore, the outliers were cleaned using the criterion of 3-sigma threshold [47], which were very few in our experimental data. Finally, because of a few of data being lost, we worked out the constant data with standard interval of 0.05 s in GNSS time series, and of 0.01 s in accelerometer time series using the linear interpolation code developed by authors. The authors developed all codes for data processing in this study with the software MATLAB (MathWorks, Natick, MA, USA) for windows version 7.0.

5.3. Identification of dynamic displacements with the MAF

The original GNSS data provide no evidence of any dynamic displacements due to errors caused by the multipath and random noise as shown in Fig. 3. To eliminate these errors in the GNSS measurements, we employed the MAF algorithm to filter the GNSS data, and designed three filtering schemes (A, B and C) with different the input data and the desired data to identify the structural dynamic displacements, respectively (Table 3). For instance, the RTK and PPK data (S_a, S_b) were employed as input and desired data in scheme A, respectively (Fig. 5a and b). To begin with, these data

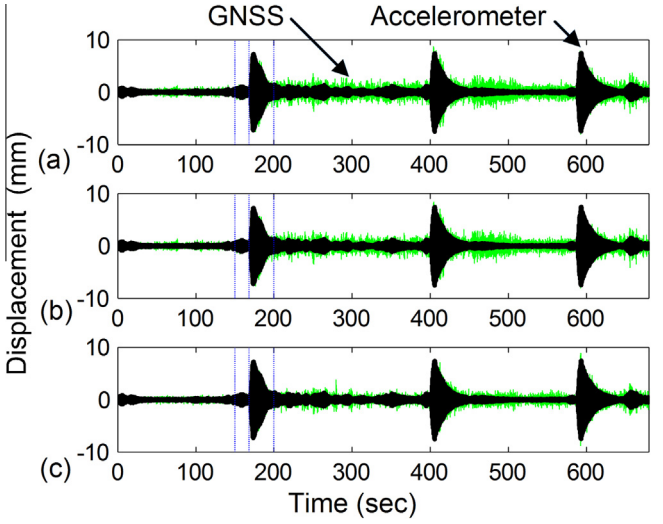

Fig. 8. Comparison of the MAF-filtered GNSS displacements with accelerometer-derived displacements. The GNSS displacements were identified from the filtering scheme A, B and C, corresponding to subfigures of (a–c), respectively.

(S_a, S_b) were filtered with the MAF, respectively, to obtain the first filtering results ($x(n)$, $d(n)$) as shown in Fig. 5c and d. Then, the results were employed as input and desired data of the LMS adaptive filtering to the obtain actual structural dynamic displacements ($y(n)$) and estimation errors ($e(n)$) as shown in Fig. 5f and e. As shown in Fig. 8, three filtering schemes (A, B and C) successfully identified the dynamic displacements of the bridge with the amplitude better than 8 mm using the multimode GNSS data. Meanwhile, The dynamic displacements were also obtained from double integration of the accelerometer-measured accelerations [48]. The drift errors were serious during the integration because of the unknown initial velocities and displacements [49]. A highpass filter with a passband frequency 1.0 Hz was employed to eliminate the drift errors. The dynamic displacements were computed from the accelerometer-measured accelerations but without semi-static component.

Both the GNSS-derived and accelerometer-derived displacements are very similar and reliable, whereas the amplitudes of the GNSS-derived displacements are larger than that of the accelerometer-derived displacements due to the residual random noise contamination of the data from the GNSS receiver. Zooming in all these subfigures in time windows of 150–200 s, it is noted that the differences of the time series of displacements between these two sensors are very small, particularly for the parts of forced vibrations (Fig. 8).

To validate the accuracy of the identified displacements, we compared the GNSS displacements extracted from these three schemes (i.e. A, B and C) with the accelerometer-derived displacements, respectively, and calculated the differences of each. The standard deviation and mean deviation values of these residuals were attained (see Table 4) corresponding to the displacements in Fig. 8. The maximum standard deviation value is ±0.8 mm while the maximum mean deviation value is 0.7 mm. In brief, all of them are less than 1 mm. The results indicates that the dynamic displacements extracted from GNSS measurements by these three filtering schemes agree well with that from accelerometer measurements, and also agree with themselves.

5.4. Extraction of modal frequencies

Each of the displacements derived from the GNSS and accelerometer measurements consists of two parts (Fig. 8). Part I in each subfigure is mainly the ambient random vibration of the bridge structure excited by wind loading and occasional pedestrian. Part

Table 4
Standard deviation (SD) and mean deviation (MD) of the residuals of the MAF-filtered GNSS displacements minus accelerometer-derived displacements.

Value	GNSS scheme A		GNSS scheme B		GNSS scheme C	
	I	II	I	II	I	II
SD (mm)	±0.2	±0.8	±0.2	±0.7	±0.2	±0.6
MD (mm)	0.2	0.7	0.1	0.6	0.1	0.4

II is mainly the forced vibration excited by the jumping of three students with an overall weight of 180 kg. The FFT was used to perform the spectral analyses since it has many successful applications in past studies. The analyzed spectrum is selected in the range of 0–5 Hz since the vibration frequencies of the bridges are mainly in the window of 0.1–5 Hz [2].

In the part I of the ambient random vibration (Fig. 10), the modal frequency of 1.680 Hz detected from the GNSS-derived displacements is identical to that from the accelerometer-derived displacements, although the peak values of the spectral magnitudes of the GNSS displacements are slightly smaller than those of the accelerometer-derived displacements. Generally, the GNSS spectral magnitudes of the whole frequency band except the peaks are larger than the accelerometer spectral magnitudes due to the more significant residuals of the random noise in the GNSS measurements than those in the accelerometer measurements.

In the part II of the forced vibration (Fig. 10), the same modal frequency of 1.690 Hz was detected by both two types of sensors. The peak values of spectral magnitudes of the GNSS-derived displacements were similar to those of accelerometer-derived displacements, whilst there exist differences in their non-peak values. Comparing the spectral magnitudes of GNSS-derived displacements in part I with those in part II, it can be found that the spectral magnitude of the peak in part II is evidently larger than that in part I because of its powerfully excited.

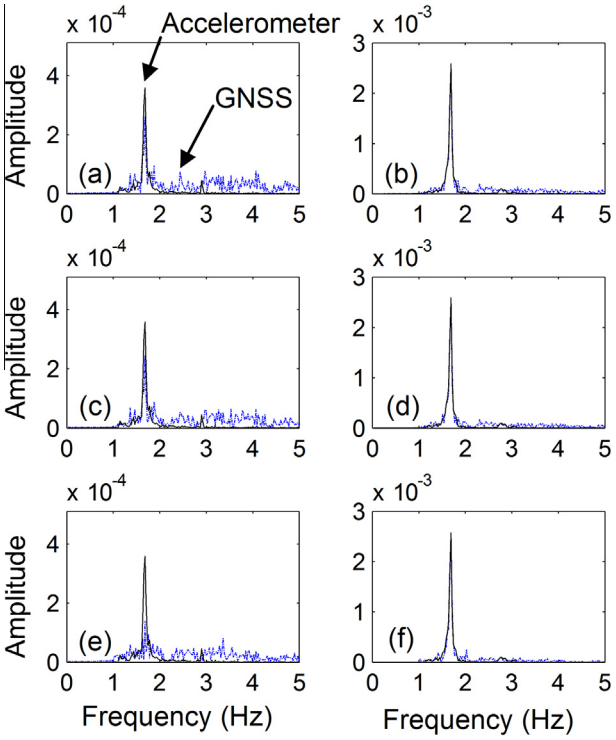

Fig. 10. Spectra corresponding to the GNSS-derived and the accelerometer-derived displacements shown in Fig. 8. The spectra of MAF-filtered GNSS results by the filtering scheme A, B and C ((a), (c), and (e)) in part I, and those in part II ((b), (d), and (f)).

5.5. Derivation of the accelerations from GNSS measurements

Another method to validate the accuracy of the GNSS-derived displacements is the comparison of the time series of accelerations computed from GNSS data with those from the accelerometer data. The GNSS-derived accelerations were computed from the GNSS data of the scheme A (Fig. 8a) by double differentiation. Additionally, the accelerometer-derived accelerations with 20 Hz sampling rate were re-sampled from the accelerometer data at 100 Hz. Both time series of acceleration derived from these two sensors were substantially identical although the GNSS-derived time series was more distinguish contaminated by the random noise

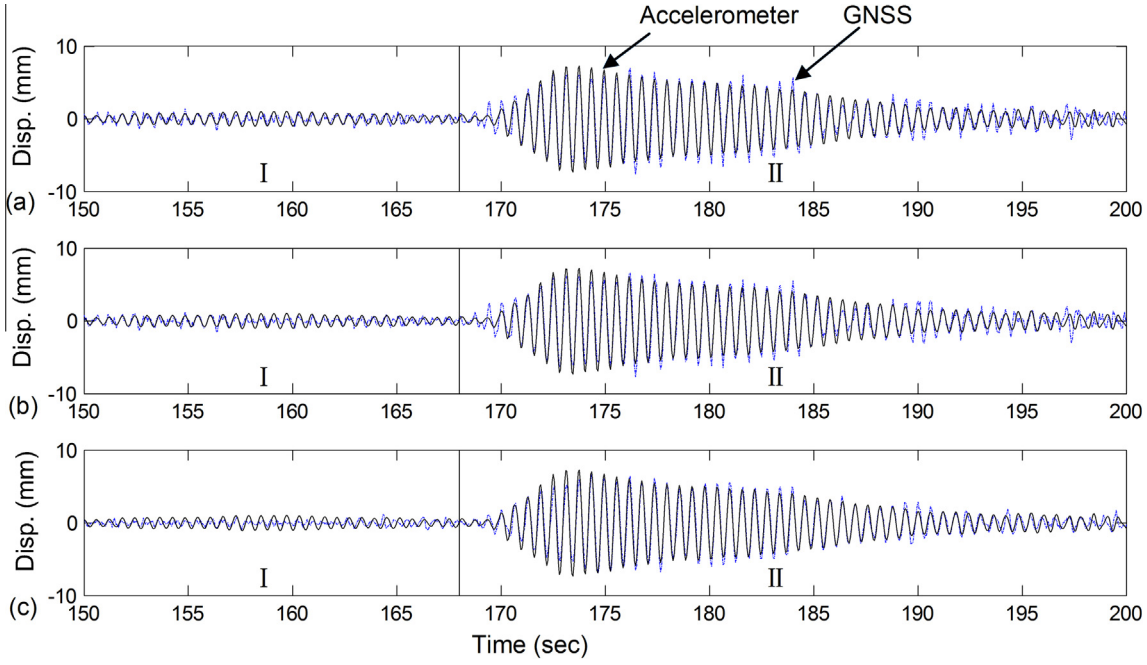

Fig. 9. The enlarged MAF-filtered-GNSS displacements and the accelerometer-derived displacements in time windows of 150–200 s in Fig. 7. The GNSS displacements were identified by the filtering scheme A, B and C, corresponding to subfigures of (a–c), respectively. Part I is ambient random vibration, and Part II is mainly forced vibration.

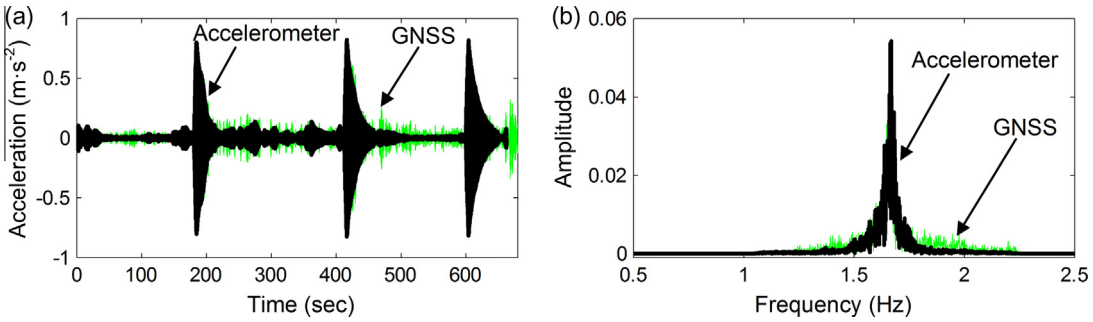

Fig. 11. Comparison of GNSS-derived accelerations with accelerometer-derived accelerations (a) and of the modal frequencies indentified from these two sets of accelerations (b).

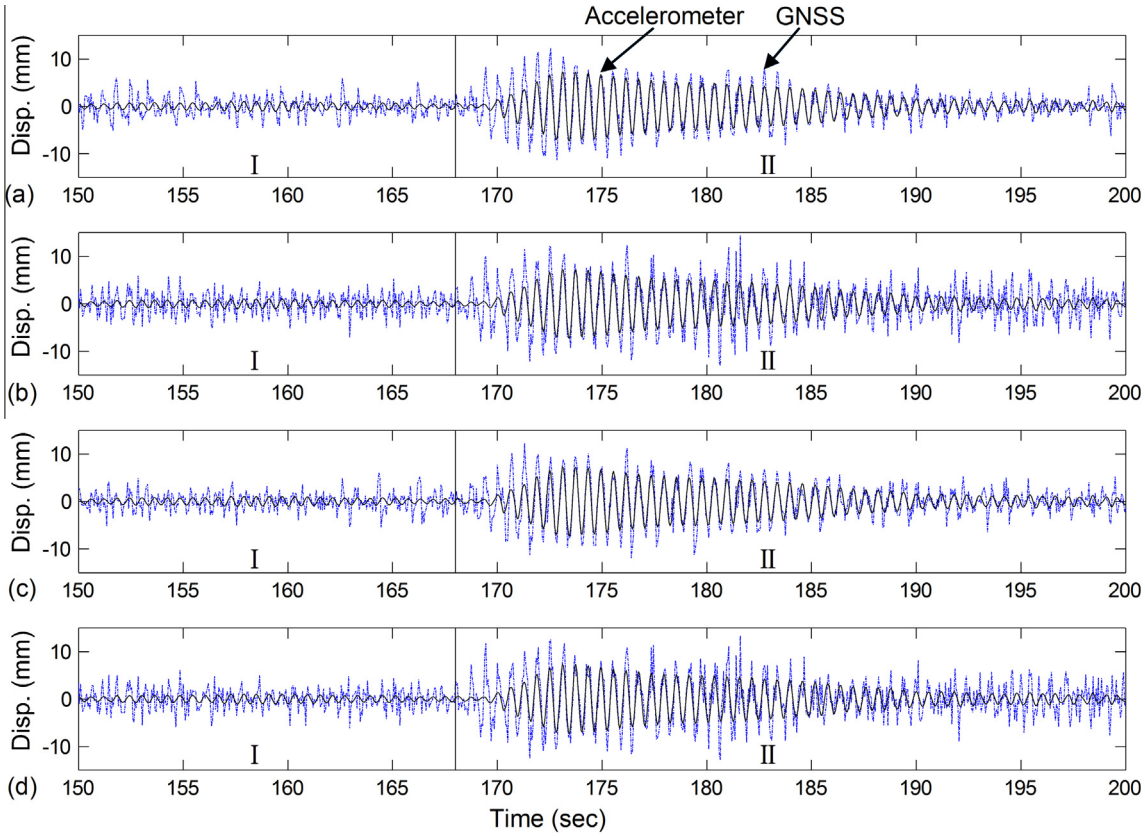

Fig. 12. Comparison of the EEMD-filtered GNSS displacements with the accelerometer-derived displacements. The GNSS-derived dynamic displacements are identified from four sets of GNSS data of S_a, S_b, S_m, S_n ((a)–(d)), with different processing mode. Part I is ambient random vibration, and Part II is mainly forced vibration.

(Fig. 11a). We calculated the differences between these two sets of accelerations. The standard deviation and mean deviation values of these differences are 0.03 m/s^2 and 0.04 m/s^2, respectively, which are good enough for monitoring purpose.

The modal frequencies identified respectively from both acceleration time series by FFT method were substantially identical with the same fundamental frequency of 1.690 Hz (Fig. 11a).

5.6. Comparison of filtering results of the MAF and the EEMD

Ensemble Empirical Mode Decomposition (EEMD) improving from the original EMD is an adaptive time–frequency data analysis method, which can accurately distinguish the signal from white noise-added data [34,50]. To compare with the MAF, we employed the EEMD method to identify the structural dynamic displacements from GNSS data. The software package of the EEMD has been developed by Flandrin's group (http://perso.ens-lyon.fr/patrick.flandrin/emd.html). Also, the similar software and its instructions can freely be downloaded from its website (http://rcada.ncu.edu.tw/research1.htm). The time series of structural vibration displacements corresponding to the four sets of GNSS multimode data (S_a, S_b, S_m, S_n) were obtained, respectively (Fig. 12).

We calculated the residuals of the time series of EEMD-filtered displacements minus those of accelerometer-derived displacements. The standard deviation and mean deviation values of these residuals were attained (Table 5). The standard deviation values vary in the range between 1.9 mm and 3.2 mm, and the mean deviation values change in the range between 1.6 mm and 2.5 mm. Furthermore, these values between in part I and II have insignificant difference, similar to among the multimode data (S_a, S_b, S_m, S_n).

Comparing the filtering results between the MAF and the EEMD (Figs. 9 and 12), it is noted that the MAF-filtered results are very

Table 5
Standard deviation (SD) and mean deviation (MD) values of the residuals of the EEMD-filtered GNSS displacement minus accelerometer-derived displacements.

Value	S_a		S_b		S_m		S_n	
	I	II	I	II	I	II	I	II
SD (mm)	±2.0	±2.1	±2.1	±3.2	±1.9	±2.3	±2.1	±3.2
MD (mm)	1.6	1.7	1.7	2.5	1.5	1.8	1.6	2.5

similar to the accelerometer-derived results while the EEMD-filtered results are obviously different from the accelerometer-derived results. Furthermore, all of the standard deviation and mean deviation values of the MAF-filtered results are less than 1 mm while those of EEMD-filtering results are larger than 1.6 mm. It seems that The MAF is more accurate and effectiveness than the EEMD.

6. Discussion and conclusion

A series of monitoring experiments were conducted on the Wilford suspension bridge in Nottingham, United Kingdom with GNSS and accelerometer sensors, in which three GNSS data acquisition modes, i.e. conventional RTK, network RTK and PPK were synchronously considered. An innovative MAF algorithm was developed to mitigate noise and identify the dynamic displacements of the bridge from the multimode GNSS data. *At a sub-millimeter level accuracy* the dynamic displacements of the bridge with the amplitude less than 8 mm were accurately identified, in close agreement with the accelerometer results. The fundamental frequency 1.690 Hz of the bridge was detected from response measurements of forced vibrations, and validated by the accelerometer results. The latest identified frequency of 1.690 Hz is slightly lower than estimated frequency 1.740 Hz by structural analysis, but the difference between these two frequencies is less than 3%, and satisfied the limitation of less than 5%. It seems that the restoration of the bridge results in the change of the fundamental frequency.

The main contribution of this study is that it is statistically validated that the GNSS positioning technology can identify the dynamic displacement at a sub-millimeter level accuracy in the case of the application of the proposed MAF algorithm. The GNSS data of three processing modes, i.e. conventional RTK, network RTK and PPK, combined in pairs can be used for structural dynamic monitoring. Taking the criterion of 3-sigma (99.7% confidence interval) as the minimum value of the detectable vibration response, GNSS positioning technology is capable of detecting the structural dynamic displacements of better than 3 mm with the MAF algorithm.

In addition, the fundamental frequency of the bridge was identified from the GNSS data, matching well with that extracted from the accelerometer dada. It seems that the GNSS positioning technology can easily and precisely detects the modal frequencies of less than 2 Hz using GNSS receivers at the sampling rate 20 Hz although the high-frequencies results (up to 4 Hz [51], even 10 Hz [23]) have achieved.

Finally, the MAF-filtered displacements are more close to the accelerometer results than the EEMD-filtered displacements. It indicates that the MAF algorithm is better than the EEMD algorithm, which has been proved versatile in many applications for extracting signals from the contaminated data [50,52]. Besides, the EEMD-filtered displacements from the network RTK GNSS data (see Fig. 12c) appears that the network RTK method can also identify the structural vibrations with relatively large noise, as well as the conventional RTK and the PPK methods.

The GNSS would therefore be a promising tool of structural health monitoring with its sampling rate and the overall performance improving significantly, complementary to accelerometers. It can be used for not only the dynamic monitoring of long-span bridges with the low vibration frequency and the large vibration amplitude, but also for the dynamic monitoring of the small and medium span bridges with the high vibration frequency and the small vibration amplitude in the case of the application of the MAF algorithm.

Acknowledgements

The authors would like to express their sincere gratitude to the University of Nottingham for supplying all experimental instruments. Thanks also go to Mr Tieshuai Li, Mr Yang Gao and Mr Sean Ince for their involvements in field experiments. This work was supported by Grant 50908083 from the National Natural Science Foundation of China.

Appendix A

The following acronyms and symbols are used in this paper:

MAF = Multimode adaptive filtering
PTDL = Precise Time Data Logger
GNSS = Global Navigation Satellite System
RTK = Real-Time Kinematic
PPK = Post-Processing Kinematic
AF = Adaptive filtering
EMD = Empirical Mode Decomposition
EEMD = Ensemble Empirical Mode Decomposition
FFT = Fast Fourier Transform
CORS = Continuously operating reference stations
S_a = Displacements derived from RTK data of GNSS receiver No. 1
S_b = Displacements derived from PPK data of GNSS receiver No. 1
S_m = Displacements derived from network RTK data of GNSS receiver No. 2
S_n = Displacements derived from PPK data of GNSS receiver No. 2
S_{acc} = Accelerations derived from accelerometer data
$M_a(n)$ = Multipath error contained in the displacements of S_a
$V_a(n)$ = Actual vibration information contained in the displacements of S_a
$N_a(n)$ = random noise contained in the displacements of S_a
$M_b(n)$ = Multipath error contained in the displacements of S_b
$V_b(n)$ = Actual vibration information contained in the displacements of S_b
$N_b(n)$ = random noise contained in the displacements of S_b
$x(n)$ = Input data during multimode adaptive filtering
$d(n)$ = Desired data during multimode adaptive filtering
$y(n)$ = Output data during multimode adaptive filtering
$e(n)$ = Estimation error during multimode adaptive filtering
$\widehat{w}_i(n)$ = Variable parameters of the adaptive filter
M = The length of the adaptive filter

References

[1] Meng X, Roberts GW, Dodson AH, Cosser E, Barnes J, Rizos C. Impact of GPS satellite and pseudolite geometry on structural deformation monitoring: analytical and empirical studies. J Geodesy 2004;77:809–22.
[2] Meng X, Dodson AH, Roberts GW. Detecting bridge dynamics with GPS and triaxial accelerometers. Eng Struct 2007;29:3178–84.
[3] Li X, Ge L, Ambikairajah E, Rizos C, Tamura Y, Yoshida A. Full-scale structural monitoring using an integrated GPS and accelerometer system. GPS Solut 2006;10:233–47.
[4] Moschas F, Stiros S. Measurement of the dynamic displacements and of the modal frequencies of a short-span pedestrian bridge using GPS and an accelerometer. Eng Struct 2011;33:10–7.
[5] Kijewski-Correa T, kareem A, Kochly M. Experimental verification and full-scale deployment of global positioning systems to monitor the dynamic response of tall buildings. J Struct Eng 2006;132:1242–53.

[6] Im SB, Hurlebaus S, Kang YJ. A summary review of GPS technology for structural health monitoring. J Struct Eng 2013;139(10):1653–64.
[7] Bonnor N. A brief history of Global Navigation Satellite Systems. J Navigat 2012;65:1–14.
[8] Lovse J, Teskey W, Cannon M. Dynamic deformation monitoring of tall structure using GPS technology. J Surv Eng 1995;121:35.
[9] Ashkenazi V, Dodson A, Moore T, Roberts G. Real time OTF GPS monitoring of the humber bridge. Surv World 1996;4:26–8.
[10] Breuer P, Chmielewski T, Gorski P, Konopka E. Application of GPS technology to measurements of displacements of high-rise structures due to weak winds. J Wind Eng Ind Aerod 2002;90:223–30.
[11] Ge L, Han S, Rizos C, Ishikawa Y, Hoshiba M, Yoshida Y, et al. GPS seismometers with up to 20 Hz sampling rate. Earth Planets Space 2000;52:881–4.
[12] Xu L, Guo JJ, Jiang JJ. Time–frequency analysis of a suspension bridge based on GPS. J Sound Vib 2002;254:105–16.
[13] Tamura Y, Matsui M, Pagnini LC, Ishibashi R, Yoshida A. Measurement of wind-induced response of buildings using RTK-GPS. J Wind Eng Ind Aerod 2002;90:1783–93.
[14] Kijewski-Correa T, Kilpatrick J, Kareem A, Kwon D-K, Bashor R, Kochly M, et al. Validating wind-induced response of tall buildings: synopsis of the Chicago full-scale monitoring program. J Struct Eng 2006;132:1509–23.
[15] Yigit CO, Li X, Inal C, Ge L, Yetkin M. Preliminary evaluation of precise inclination sensor and GPS for monitoring full-scale dynamic response of a tall reinforced concrete building. J Appl Geodesy 2010;4:103–13.
[16] Watson C, Watson T, Coleman R. Structural monitoring of cable-stayed bridge: analysis of GPS versus modeled deflections. J Surv Eng 2007;133:23–8.
[17] Robert GW, Brown C, Meng X. Deflection and frequency monitoring of forth road bridge, Scotland, by GPS. Proc ICE-Bridge Eng 2012;165:105–23.
[18] Meng X. Real-time deformation monitoring of bridges using GPS/accelerometers, PhD dissertation. Nottingham: The University of Nottingham; 2002.
[19] Li X, Rizos C, Ge Li, Tamura Y, Yoshida A. The complementary characteristics of GPS and accelerometer in monitoring structural deformation. In: Proceedings of the U.S. institute of navigation national technical meeting. San Diego; 2005. P. 911–20.
[20] Yi T, Li H, Gu M. Full-scale measurements of dynamic response of suspension bridge subjected to environmental loads using GPS technology. Sci China Ser E 2010;53:469–79.
[21] Moschas F, Stiros SC. Three-dimensional dynamic deflections and natural frequencies of a stiff footbridge based on measurements of collocated sensors. Struct Control Health Monit 2014;21:23–42.
[22] Nickitopoulou A, Protopsalti K, Stiros S. Monitoring dynamic and quasi-static deformations of large flexible engineering structures with GPS: accuracy, limitations and promises. Eng Struct 2006;28:1471–82.
[23] Yi TH, Li HN, Gu M. Experimental assessment of high-rate GPS receivers for deformation monitoring of bridge. Measurement 2013;46:420–32.
[24] Roberts GW, Cosser E, Meng X, Dodson AH. High frequency deflection monitoring of bridges by GPS. J Glob Pos Syst 2004;3:226–31.
[25] Chan WS, Xu YL, Ding XL, Xiong YL, Dai WJ. Assessment of dynamic measurement accuracy of GPS in three directions. J Surv Eng 2006;132:108–17.
[26] Moschas F, Stiros SC. PLL bandwidth and noise in 100 Hz GPS measurements. GPS Solut; 2014. p. 1–13 [Published online].
[27] Moschas F, Stiros S. Dynamic multipath in structural bridge monitoring: an experimental approach. GPS Solut. 2014;18:209–18.
[28] Yi TH, Li HN, Gu M. Recent research and applications of GPS based technology for bridge health monitoring. Sci China Ser E 2010;53:2597–610.
[29] Ogaja C, Li X, Rizos C. Advances in structural monitoring with global positioning system technology: 1997–2006. J Appl Geod 2007;1:171–9.
[30] Zheng D, Zhong P, Ding X, Chen W. Filtering GPS time-series using a Vondrak filter and cross-validation. J Geodesy 2005;79:363–9.
[31] Ge L, Han S, Rizos C. Multipath mitigation of continuous GPS measurements using an adaptive filter. GPS Solut 2000;4:19–30.
[32] Ge L, Han S, Rizos C. GPS multipath change detection in permanent GPS stations. Surv Rev 2002;36:306–22.
[33] Roberts GW, Meng X, Dodson AH. Using adaptive filtering to detect multipath and cycle slips in GPS/accelerometer bridge deflection monitoring data. In: Proceedings of XXII international congress of the FIG. Washington DC (USA); 2002 April 19–26.
[34] Chan W, Xu Y, Ding X, Dai W. An integrated GPS–accelerometer data processing technique for structural deformation monitoring. J Geodesy 2006;80:705–19.
[35] Yi TH, Li HN, Gu M. Characterization and extraction of global positioning system multipath signals using an improved particle-filtering algorithm. Meas Sci Technol 2011;22:1–11.
[36] Psimoulis PA, Stiros SC. A supervised learning computer-based algorithm to derive the amplitude of oscillations of structures using noisy GPS and Robotic Theodolites (RTS) records. Comput Struct 2012;92:337–48.
[37] Yi TH, Li HN, Gu M. Wavelet based multi-step filtering method for bridge health monitoring using GPS and accelerometer. Smart Struct Syst 2013;11:331–48.
[38] Roberts GW, Meng X, Dodson AH. Integrating a global positioning system and accelerometers to monitor the deflection of bridges. J Surv Eng 2004;130:65–8.
[39] Cosser E, Roberts GW, Meng X, Dodson A. Measuring the dynamic deformation of bridges using a total station. In: Stiros S, Pytharouli S, editors. 11th FIG symposium on deformation measurements. Santorini: Patras University; 2003. p. 605–12.
[40] Meo M, Zumpano G, Meng X, Cosser E, Roberts G, Dodson A. Measurements of dynamic properties of a medium span suspension bridge by using the wavelet transforms. Mech Syst Signal Pr 2006;20:1112–33.
[41] Tolman BW, Craig BK. An integrated GPS/accelerometer system for low dynamics applications. In: Proceedings of the international symposium on kinematic systems in geodesy, geomatics, and navigation. Banff, Canada; 1997 [June 3–6].
[42] Meng X, Gogoi N, Dodson AH, Roberts GW, Brown CJ. Using Multi-constellation GNSS and EGNOS for bridge deformation monitoring. In: Proceedings of the joint international symposium on deformation monitoring. Hong Kong, China; 2011 [November 2–4].
[43] Edwards S, Clarke P, Penna N, Goebell S. An examination of network RTK GPS services in Great Britain. Surv Rev 2010;42:107–21.
[44] Moschas F, Stiros S. Noise characteristics of high-frequency, short-duration GPS records from analysis of identical, collocated instruments. Measurement 2013;46:1488–506.
[45] Ge L, Chen HY, Han S, Rizos C. Adaptive filtering of continuous GPS results. J Geodesy 2000;74:572–80.
[46] Haykin S. Adaptive filter theory. 3rd ed. Upper Saddle River (NJ): Prentice-Hall; 1996.
[47] Stiros SC, Psimoulis PA. Response of a historical short-span railway bridge to passing trains: 3-D deflections and dominant frequencies derived from Robotic Total Station (RTS) measurements. Eng Struct 2012;45:362–71.
[48] Park KT, Kim SH, Park HS, Lee KW. The determination of bridge displacement using measured acceleration. Eng Struct 2005;27:371–8.
[49] Stiros SC. Errors in velocities and displacements deduced from accelerographs: an approach based on the theory of error propagation. Soil Dyn Earthquake Eng 2008;28:415–20.
[50] Wu Z, Huang NE. Ensemble empirical mode decomposition: a noise-assisted data analysis method. Adv Adapt Data Anal 2009;1:1–41.
[51] Psimoulis P, Pytharouli S, Karambalis D, Stiros S. Potential of Global Positioning System (GPS) to measure frequencies of oscillations of engineering structures. J Sound Vib 2008;318:606–23.
[52] Huang NE, Wu Z. Hilbert-Huang transform and its applications. Singapore: World Scientific; 2005.